Electronic Supplementary Material (ESI) for Journal of Materials Chemistry A.

Electronic supplementary information (ESI)

A facile method for the synthesis of graphene-like 2D metal oxides and their excellent catalytic application in the hydrogenation of nitroarenes

Lijun Lei,[a,b] Zhiwei Wu*,[a] Huan Liu,[a,b] Zhangfeng Qin,*,[a] Chengmeng Chen,[c] Li Luo,[a,b] Guofu Wang,[a] Weibin Fan,[a] and Jianguo Wang*,[a]

[a] *State Key Laboratory of Coal Conversion, Institute of Coal Chemistry, Chinese Academy of Sciences, P.O. Box 165, Taiyuan, Shanxi 030001, PR China*

[b] *University of the Chinese Academy of Sciences, Beijing 100049, PR China*

[c] *Key Laboratory of Carbon Materials, Institute of Coal Chemistry, the Chinese Academy of Sciences, Taiyuan 030001, PR China*

* *Corresponding authors. Tel.: +86-351-4046092; Fax: +86-351-4041153. E-mail address: qzhf@sxicc.ac.cn (Z. Qin); iccjgw@sxicc.ac.cn (J. Wang); wuzhiwei@sxicc.ac.cn (Z. Wu)*

As the Electronic supplementary information (ESI) of the manuscript "*A facile method for the synthesis of graphene-like 2D metal oxides and their excellent catalytic application in the hydrogenation of nitroarenes*", following materials are provided:

(1) More experimental details for the preparation of GO, and various 2D metal oxides nanosheets;

(2) More results including the SEM images, TEM images, XRD patterns, N_2 adsorption and desorption isotherms, Raman spectra, XPS spectra, and H_2-TPR profiles of various CeO_2 and other metal oxides samples; the TG curves and EDX elemental mapping analysis of GO-Ce complexes; the catalytic reaction results for the hydrogenation of nitroarenes over Pd/NS-CeO_2-450 conducted in different solvents and with different hydrogen sources; the catalytic performance of various metals supported on NS-CeO_2 in the hydrogenation of nitrobenzene; the TEM images, H_2-TPR profiles, Pd 3d XPS spectra, and Pd K-edge EXAFS spectra of various Pd/NS-CeO_2 catalysts.

1. More experimental details

Preparation of graphene oxide (GO). GO was synthesized by a modified Hummers' method.[1] Briefly, graphite powder (10 g) and sodium nitrate (5 g) were mixed with sulfuric acid (98 wt.%, 230 mL) in a beaker immersed in an ice-water bath with agitation. Potassium permanganate (30 g) was then added slowly to the mixture and the resultant mixture was kept at 35±2 °C for 30 min. After that, deionized water (460 mL) was added gradually; the water bath temperature was then increased to 98 °C and maintained at this temperature for 40 min. The resultant bright-yellow suspension was then diluted and further treated with H_2O_2 solution (30%, 30 mL). Finally, the suspension was centrifuged and washed carefully to remove the residual salt, and then dewatered at 50 °C under vacuum to obtain the graphite oxide powder. Graphene oxide was then obtained by exfoliating the graphite oxide in aqueous solution under sonication for 2 h, and followed by a vacuum drying process.

Preparation of various metal oxides nanosheets. The method for preparing all other metal oxides nanosheets is similar to that for NS-CeO_2-450, as described in the main manuscript. For the preparation of NS-TiO_2, the mixture of a certain amount of tetrabutyl titanate ($Ti(OC_4H_9)_4$) and 2 mL HNO_3 (1 mol L^{-1}) was added in ethanol with dispersed GO sheets. The molar ratios of Ce/M in all binary Ce-M metal oxides are 8 in this work.

2. More detailed results:

Table S1 Surface area, pore size, crystal size, and cell parameter of various ceria samples obtained by N_2 adsorption-desorption and XRD analysis

Entry	Sample	Surface area (m^2/g)	Pore size (nm)	Crystal size (nm) [a]	Cell parameter (Å) [b]
1	GO-Ce-80	10.8	--	--	--
2	GO-Ce-200	11.2	--	--	--
3	GO-CeO_2-300	118.3	4.4	6.7	5.468
4	NS-CeO_2-450	83.5	4.6	7.4	5.467
5	NS-CeO_2-600	49.1	9.1	8.8	5.414
6	NS-CeO_2-700	20.5	23.2	14.9	5.412
7	NS-CeO_2-850	4.2	--	49.8	5.409
8	GO	36.4	--	--	--
9	B-CeO_2	61.5	5.9	10.7	5.410

[a] Average CeO_2 crystal sizes were estimated from the broadening of CeO_2 (111), (200), (220), and (113) diffraction peaks by using the Scherrer formula from the XRD patterns of corresponding CeO_2 samples.

[b] Cell parameter were calculated from the CeO_2 planes (111), (200), (220), and (113) by the MDI Jade software.

Table S2 Content of Ce^{3+} in different CeO_2 samples

Entry	Sample	Ov/F_{2g} [a]	Ce^{3+} in CeO_2 (%) [b]	Ce^{3+} on the surface (%) [c]
1	NS-CeO_2-450	0.261	20.7	23.2
2	NS-CeO_2-600	0.227	18.5	19.7
3	NS-CeO_2-700	0.191	16.0	18.1
4	NS-CeO_2-850	0.146	12.7	14.8
5	B-CeO_2	0.149	13.0	15.0

[a] The Ov/F_{2g} ratio is obtained from the Raman spectra.

[b] The content of Ce^{3+} in CeO_2 is calculated by $Ov/(F_{2g} + Ov)\times 100\%$, from the Raman spectra.

[c] The content of Ce^{3+} on the CeO_2 surface is determined by the Ce 3d XPS spectra, as described by Li and co-workers.[2]

Table S3 Reduction peak position and area of reducible surface and bulk CeO_2 species derived from the H_2-TPR profiles of various CeO_2 samples

Entry	Sample	Peak position (°C)		Peak area (a.u.)		$A_{\mathrm{surface}}/(A_{\mathrm{bulk}}+A_{\mathrm{surface}})$ (%)
		Surface	Bulk	Surface	Bulk	
1	NS-CeO_2-450	528	785	27646	1301	95.5
2	NS-CeO_2-600	521	793	13146	1495	89.8
3	NS-CeO_2-700	482	820	4533	2493	64.5
4	NS-CeO_2-850	452	827	1167	4657	20.0
5	B-CeO_2	447	820	1431	3772	27.5

Note: A_{surface} represents the integration area in the H_2-TPR profiles for the reduction of surface-related CeO_2 species, whereas A_{bulk} refers to that for the reduction of bulk CeO_2 species.

Table S4 Stoichiometric data of various NS-CeO_2 samples at different temperatures

Entry	Sample	Content of surface Ce^{3+} (%) [a]	Surface O/Ce ratio [a]	Residual C (wt.%) [b]	Residual S (wt.%) [b]
1	NS-CeO_2-300	27.8	1.86	4.58	2.96
2	NS-CeO_2-400	25.4	1.87	2.34	1.92
3	NS-CeO_2-450	23.2	1.88	0.42	0.41
4	NS-CeO_2-600	19.7	1.90	0.22	0.32
5	NS-CeO_2-700	18.1	1.91	0.13	0.28
6	NS-CeO_2-850	14.8	1.93	0.10	0.13

[a] The surface fraction of Ce^{3+} and Ce/O ratio were derived from the XPS results.

[b] The content of residual C and S from GO were determined by elemental microanalysis.

Table S5 Main parameters of other 2D metal oxides prepared through modified EISA method in this work

Entry	Sample	Elemental ratio [a]	Residual C (wt.%) [b]	Residual S (wt. %) [b]	Thickness (nm) [d]
1	NS-TiO_2	--	0.74	0.58	3.6
2	NS-ZrO_2	--	0.82	0.64	4.6
3	NS-NiO	--	0.63	0.59	7.4
4	NS-CoO_x	--	0.76	0.84	6.0
5	NS-CuO	--	0.54	0.47	6.2
6	NS-Al_2O_3	--	0.20	1.52	5.5
7	NS-Cr_2O_3-ZnO	Cr:Zn = 1.18:1	0.13	1.24	9.7
8	NS-MnO_2-Al_2O_3	Mn:Al = 0.82:1	0.59	0.38	10.2
9	NS-CuO-ZrO_2	Cu:Zr = 1.16:1	0.82	1.05	6.5
10	NS-FeO_x-CoO_x	Fe:Co = 1.04:1	0.67	0.53	3.9
11	NS-CeO_2-CuO	Ce:Cu = 7.03:1	0.21	0.84	6.5
12	NS-CeO_2-CoO_x	Ce:Co = 8.12:1	0.51	1.06	7.9
13	NS-CeO_2-NiO	Ce:Ni = 6.95:1	0.13	1.01	8.2
14	NS-CeO_2-ZrO_2	Ce:Zr = 4.25:1	0.06	0.85	7.5
15	NS-CeO_2-ZnO	Ce:Zn = 1.83:1	0.10	0.74	7.8
16	NS-CeO_2-TiO_2	Ce:Ti = 4.59:1	0.07	0.55	5.7
17	NS-CeO_2-MnO_x	Ce:Mn = 3.80:1	0.04	0.73	6.3
18	NS-CeO_2-La_2O_3	Ce:La = 3.30:1	0.14	0.96	5.4
19	NS-CeO_2-Cr_2O_3	Ce:Cr = 7.64:1	0.04	0.63	4.9
20	NS-CeO_2-Al_2O_3	Ce:Al = 6.53:1	0.21	1.21	8.2
21	NS-CeO_2-FeO_x	Ce:Fe = 7.64:1	0.32	0.83	7.6
22	NS-CuO-CeO_2-ZrO_2	Cu:Ce:Zr = 1.13:1.42:1	0.12	1.33	6.5
23	NS-MnO_x-CeO_2-ZrO_2	Mn:Ce:Zr = 2.36:1.75:1	0.08	0.94	6.1

[a] The elemental ratio of various metals were determined by ICP-OES.

[b] The content of residual C and S from GO were determined by elemental microanalysis.

[d] The sheet thickness of various 2D metal oxides were measured from their TEM images.

Table S6 Comparison of various catalysts in their performance for the hydrogenation of nitrobenzene to aniline

Catalyst	NB/metal mol. ratio	Solvent	Time (h)	Conv. (%)	Sel. (%)	Yield (%)	TON	TOF (h^{-1})	Ref.
Pd/PEG	178	EtOH	3	84	91		50	126	3
Pd/PVDF	8	H_2O	2.5	100	98		3	-	4
Pd/MONT	200	THF	1	99	99		200	-	5
Pd-AmP-MCF	200	EtOAc	0.75	-	-	90	266	-	6
Fe_3O_4-NH_2-Pd	64	EtOH	0.75	-	-	99	85	-	7
Pd-MLF-11	145	MeOH/H_2O	0.5	-	-	99	290	-	8
Pt-PICP	200	THF	1	100	99		200	-	9
Pd-pol	57	H_2O	6	-	-	96	10	-	10
Pt-SiO_2	200	MeOH	1	100	100		200	-	11
Pd/NiO-M	100	EtOH	1	-	-	99	100	-	12
Pd/NS-CeO_2-450	1300	MeOH	1	100	100		1300	3010	This work

Table S7 Hydrogenation of nitrobenzene (NB) over the Pd/NS-CeO_2-450 catalyst using various hydrogen sources

Entry	Hydrogen source	Temperature (°C)	Time (h)	Conversion (%)	Selectivity (%)
1 [a]	Hydrazine hydrate	40	3	99.8	>99.9
2 [b]	Isopropanol	50	2.5	99.6	>99.9
3 [c]	hydrogen	25	1	>99.9	>99.9

[a] 5 mg Pd/NS-CeO_2 catalyst, a certain amount of NB and hydrazine hydrate (N_2H_4), and 5 mL methanol were loaded; the molar ratios of NB/Pd and N_2H_4/NB were about 650 and 3, respectively; the reaction was carried out at 0.2 MPa Ar, 40 °C, and with agitation (300 rpm).

[b] 5 mg Pd/NS-CeO_2 catalyst, a certain amount of NB and KOH, and 5 mL isopropanol were loaded; the molar ratios of NB/Pd and KOH/NB were about 650 and 5, respectively; the reaction was carried out at 0.2 MPa Ar, 50 °C, and with agitation (300 rpm). After the reaction, the pH value of mixed solution was adjusted to neutral with 0.2 mol L^{-1} HCl.

[c] 5 mg Pd/NS-CeO_2 catalyst, a certain amount of NB, and 5 mL methanol were loaded; the molar ratio of substrate/Pd was about 1300; the reaction was carried out at 0.2 MPa H_2, 25 °C, and with agitation (300 rpm).

Table S8 Solvent effect on the catalytic hydrogenation of nitrobenzene (NB) to aniline (AN) over the Pd/NS-CeO_2-450 catalyst

Entry [a]	Solvent	NB conversion (%)	Selectivity to AN(%)
1	Carbon dichloride	2.7	>99.9
2	Cyclohexane	4.6	>99.9
3	1,4-Dioxane	17.1	65.4
4	Ethyl acetate	27.5	79.6
5	Acetone	64.9	89.6
6	Toluene	68.1	98.9
7	Isopropanol	99.5	> 99.9
8	Methanol	> 99.9	> 99.9
9	Water	> 99.9	> 99.9
10 [b]	Solvent-free	> 99.9	> 99.9

[a] For Entries 1–9: 5 mg Pd/NS-CeO_2 catalyst, a certain amount of NB, and 5 mL solvent were loaded; the molar ratio of substrate/Pd was about 1300; the reaction were carried out 0.2 MPa H_2, 25 °C, and with agitation (300 rpm).

[b] For Entry 10: 20 mg Pd/NS-CeO_2 catalysts and 3 g NB were loaded; the reaction was carried out at 0.2 MPa H_2, 25 °C, and with agitation (300 rpm).

Table S9 Results of Pd K-edge EXAFS spectra fitted for various Pd/NS-CeO$_2$ samples

Sample	Shell	CN	N_{total}	R (Å)	ΔE (eV)	σ^2 (Å^2)	R-factor
Pd/NS-CeO$_2$-450	Pd–O	1.0 (±0.2)	5.6	2.04 (±0.02)	10.20	0.001	0.0061
	Pd–Pd	4.6 (±0.7)		2.75 (±0.01)	0.29	0.006	
Pd/NS-CeO$_2$-300	Pd–O	1.5 (±0.1)	4.4	1.99 (±0.01)	8.04	0.001	0.0025
	Pd–Pd	2.9 (±0.3)		2.73 (±0.01)	0.06	0.006	
Pd/NS-CeO$_2$-500	Pd–O	2.2 (±0.2)	4.5	2.02 (±0.01)	9.12	0.001	0.0199
	Pd–Pd	2.3 (±0.2)		2.72 (±0.03)	0.70	0.008	
Pd/NS-CeO$_2$-450 (calcined at 300 °C)	Pd–O	2.6 (±0.2)	2.6	1.99 (±0.01)	6.98	0.002	0.0143
	Pd–Pd	-		-	-	-	
Pd/NS-CeO$_2$-450 (calcined at 300 °C)	Pd–O	2.7 (±0.1)	2.7	1.99 (±0.01)	7.15	0.001	0.0032
	Pd–Pd	-		-	-	-	

Note: CN, coordination number; ΔE, inner core correction; R, distances; σ^2, Debye-Waller Factor. (Fit range $3 < k < 11$, $1.2 < R < 3.2$, number of independent points = 9.5)

Table S10 State of Pd species for various Pd/NS-CeO_2 catalysts determined by XPS

Entry	Catalyst	Pd^0 peak area		Pd^{2+} peak area		Pd^0 fraction (%)
		$3d_{5/2}$	$3d_{3/2}$	$3d_{5/2}$	$3d_{3/2}$	
1	Pd/NS-CeO_2-450	1343	1122	1151	1041	52.9
2	Pd/NS-CeO_2-300	1159	968	1137	1029	49.5
3	Pd/NS-CeO_2-500	734	581	1078	858	40.4
4	Pd/NS-CeO_2-450 (calcined at 300 °C)	--	--	1358	1079	0
5	Pd/NS-CeO_2-450 (calcined at 500 °C)	--	--	1579	1271	0

Note: Pd^0 fraction = (Pd^0 $3d_{5/2}$ + Pd^0 $3d_{3/2}$)/(Pd^0 $3d_{5/2}$ + Pd^0 $3d_{3/2}$ + Pd^{2+} $3d_{5/2}$ + Pd^{2+} $3d_{3/2}$)

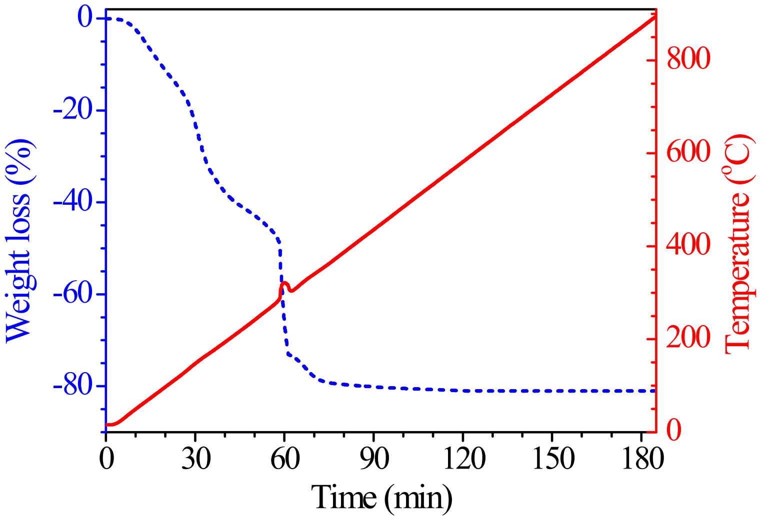

Fig. S1 Thermogravimetric (TG) curve of the GO-Ce-80 complex.

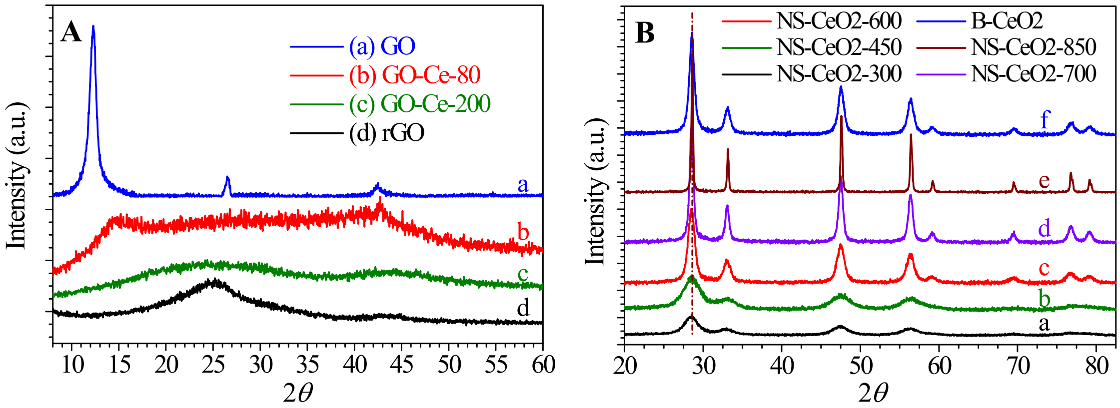

Fig. S2 XRD patterns of various GO and CeO_2 samples. (A) (a) GO; (b) GO-Ce-80; (c) GO-Ce-200; and (d) rGO. (B) (a) GO-Ce-300; (b) NS-CeO_2-450; (c) NS-CeO_2-600; (d) NS-CeO_2-700; (e) NS-CeO_2-850; and (f) B-CeO_2.

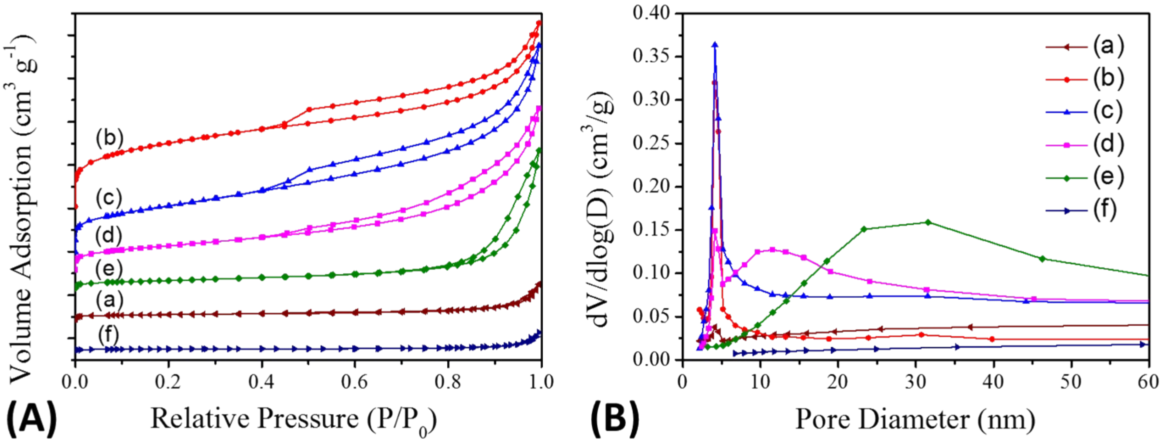

Fig. S3 (A) N_2 adsorption-desorption isotherms and (B) pore size distribution curves of various CeO_2 samples. (a) GO-Ce-200, (b) GO-Ce-300, (c) NS-CeO_2-450, (d) NS-CeO_2-600, (e) NS-CeO_2-700, and (f) NS-CeO_2-850.

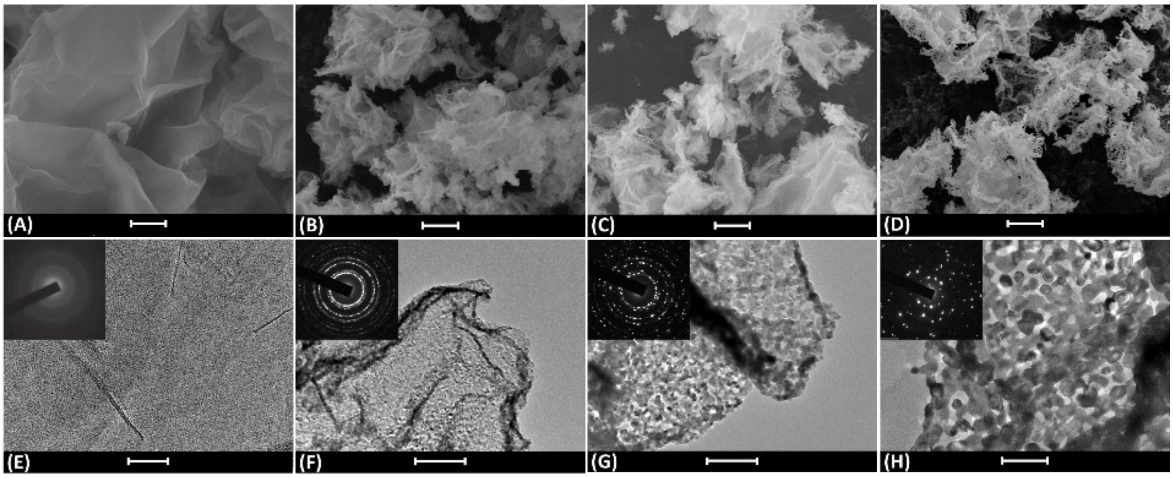

Fig. S4 SEM images of (A) GO-Ce-80, (B) NS-CeO_2-600, (C) NS-CeO_2-700, and (D) NS-CeO_2-850, TEM images of (E) GO-Ce-80, (F) NS-CeO_2-600, (G) NS-CeO_2-700, and (H) NS-CeO_2-850. The insets of (E), (F), (G), and (H) are electron diffraction (SAED) pattern in the selected area of correspond samples. Scale bars: (A–D) 1 µm, (E–H) 200 nm.

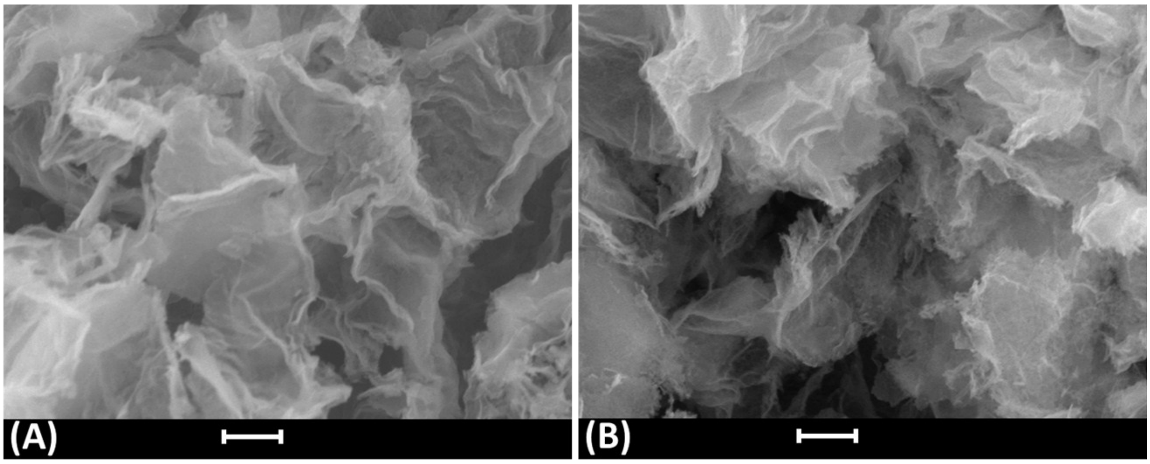

Fig. S5 SEM images of the 2D porous NS-CeO_2 samples synthesized with different Ce precursors: (A) $CeCl_3$; and (B) $Ce(NH_4)_2(NO_3)_6$. Scale bar is for 1 μm.

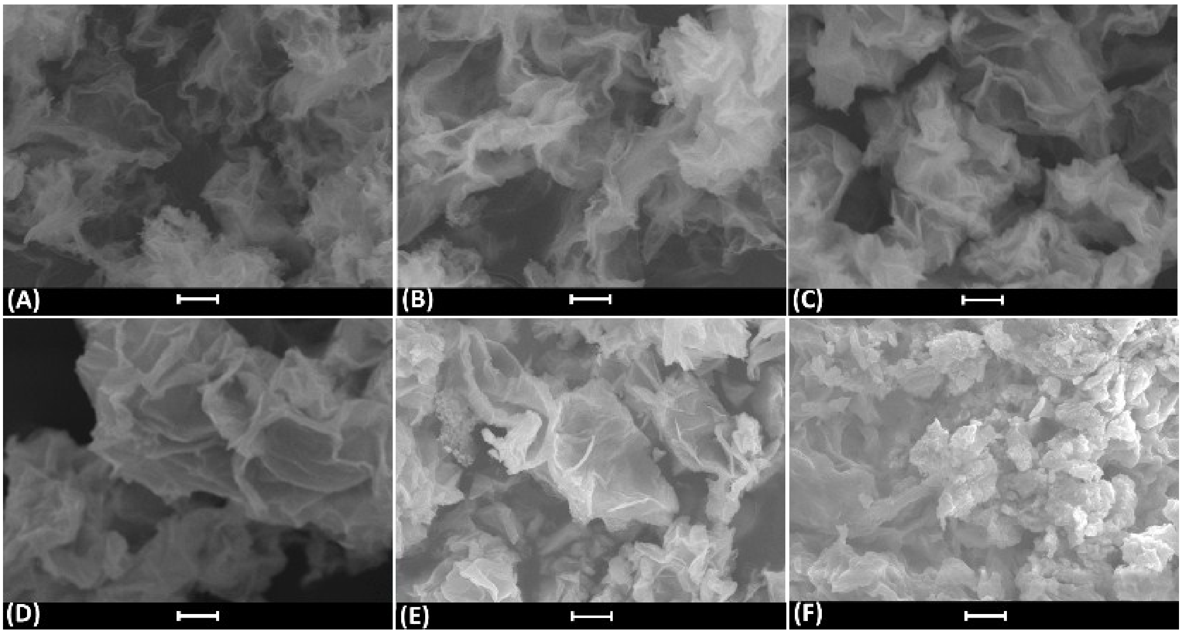

Fig. S6 SEM images of the 2D porous NS-CeO_2 samples synthesized with different mass ratios of GO and Ce: (A) 2; (B) 1; (C) 1/2; (D) 1/3; (E) 1/4; and (F) 1/8. Scale bar is for 1 μm.

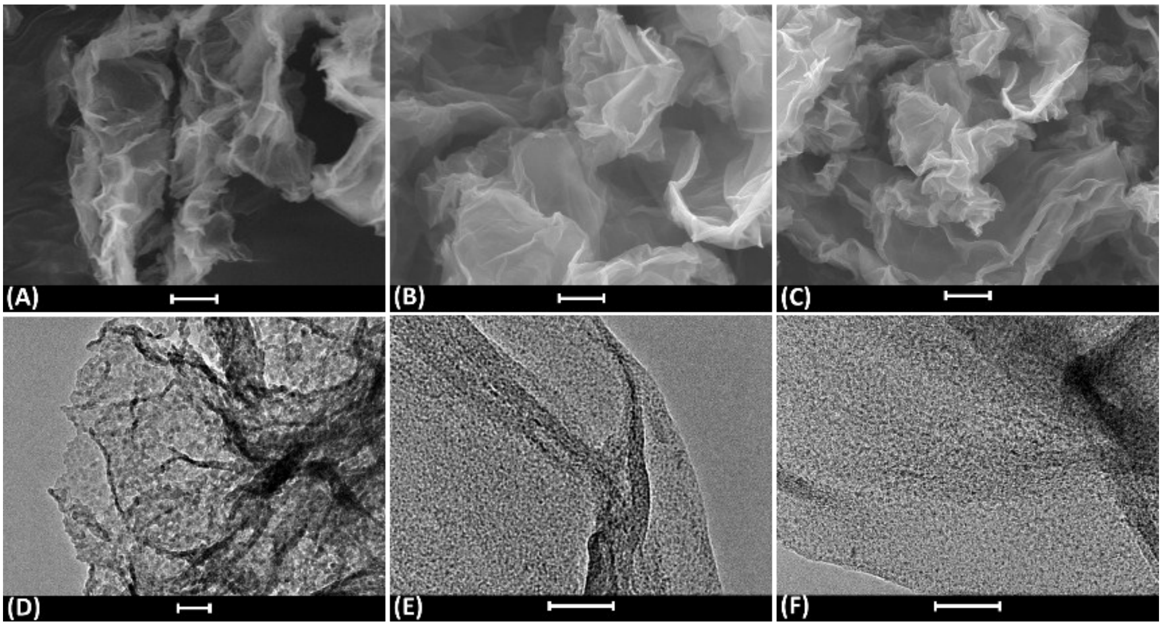

Fig. S7 SEM and TEM images of the GO-Ce sheets calcined at 450 °C in different atmospheres (20 mL min^{-1}): (A), (D) in O_2; (B), (E) in Ar; and (C), (F) in H_2. Scale bar: (A–C) 1 μm, and (D–F) 50 nm.

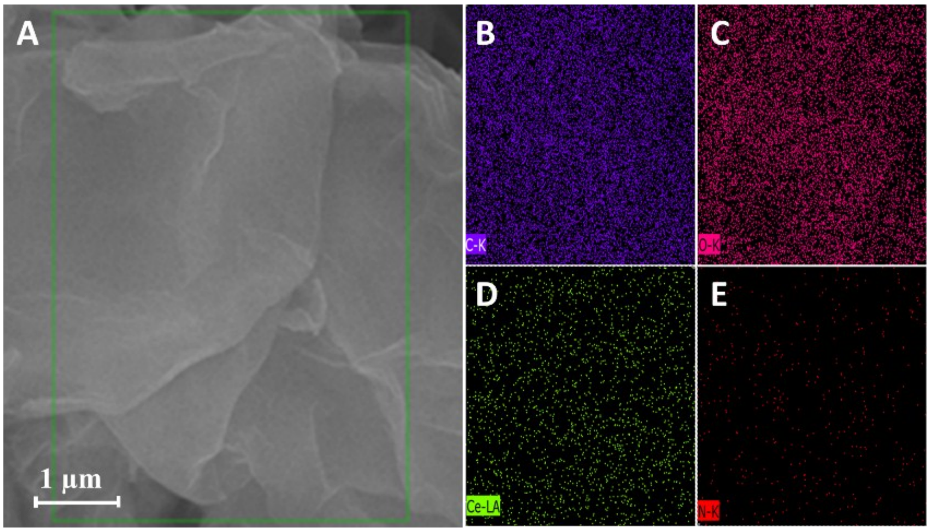

Fig. S8 EDX elemental mapping images of a GO-Ce complex sheet.

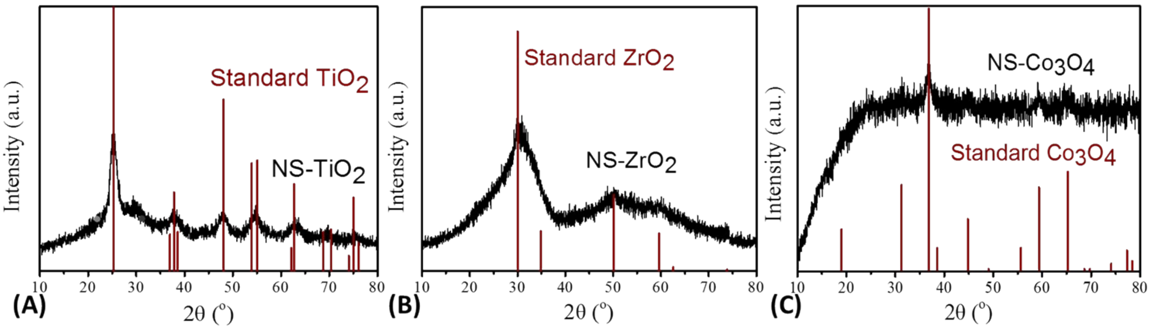

Fig. S9 XRD patterns of the 2D nanosheets of TiO_2, ZrO_2, and Co_3O_4.

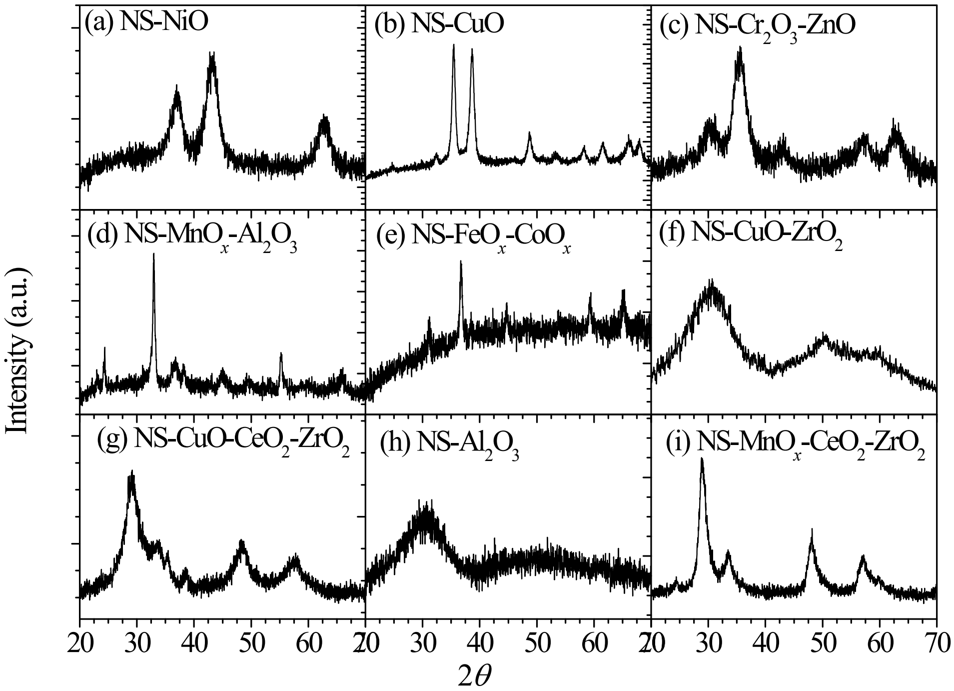

Fig. S10 XRD patterns of various 2D metal oxides nanosheets. For bimetal oxides and multicomponent metal oxides, equimolar quantities of different metal precursors were used.

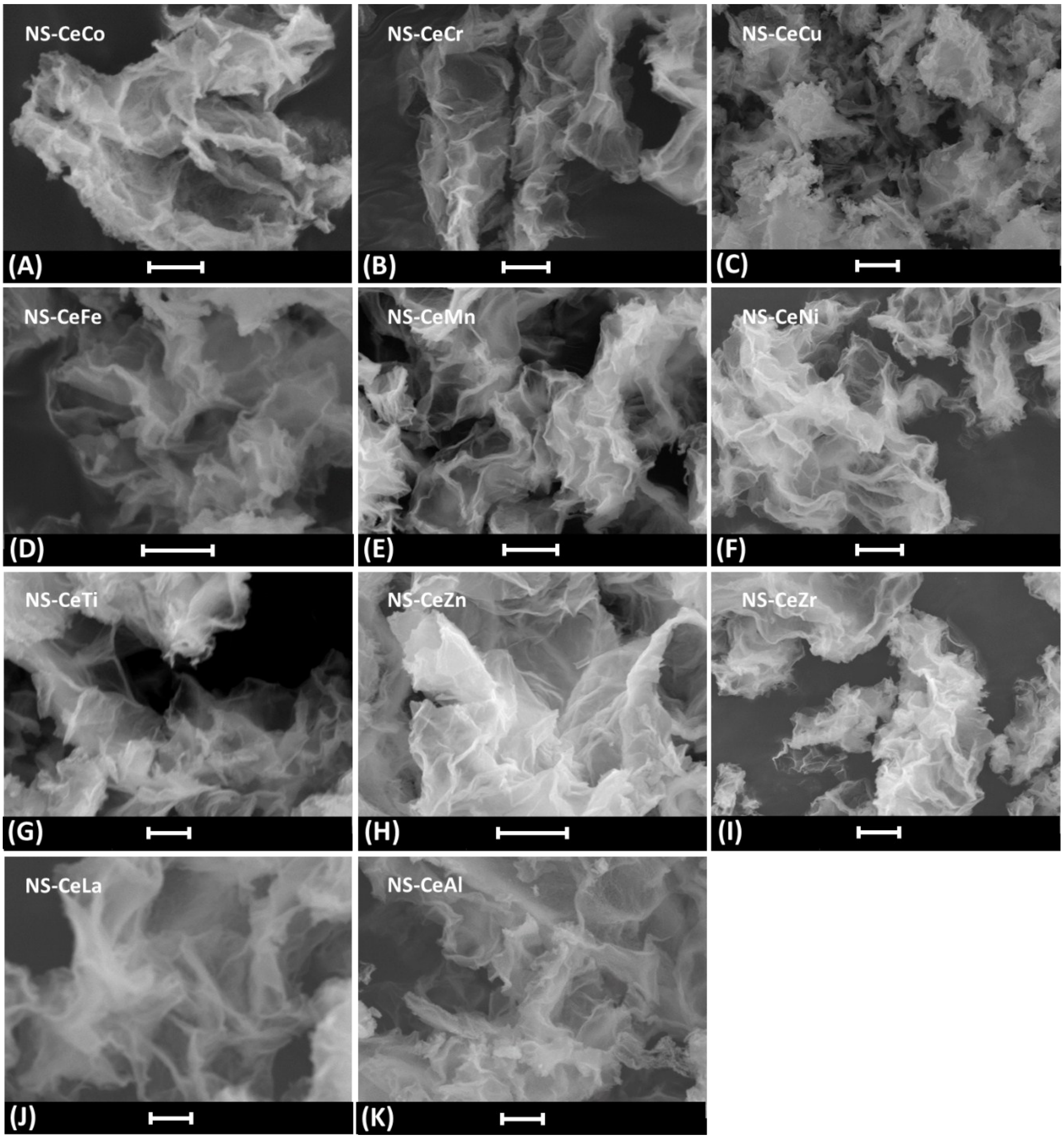

Fig. S11 SEM images of 2D porous NS-CeCo (A), NS-CeCr (B), NS-CeCu (C), NS-CeFe (D), NS-CeMn (E), NS-CeNi (F), NS-CeTi (G), NS-CeZn (H), NS-CeZr (I), NS-CeLa (J), and NS-CeAl (K). Scale bar is for 0.5 μm. In all the CeM samples, the molar ratio of Ce/M is 8.

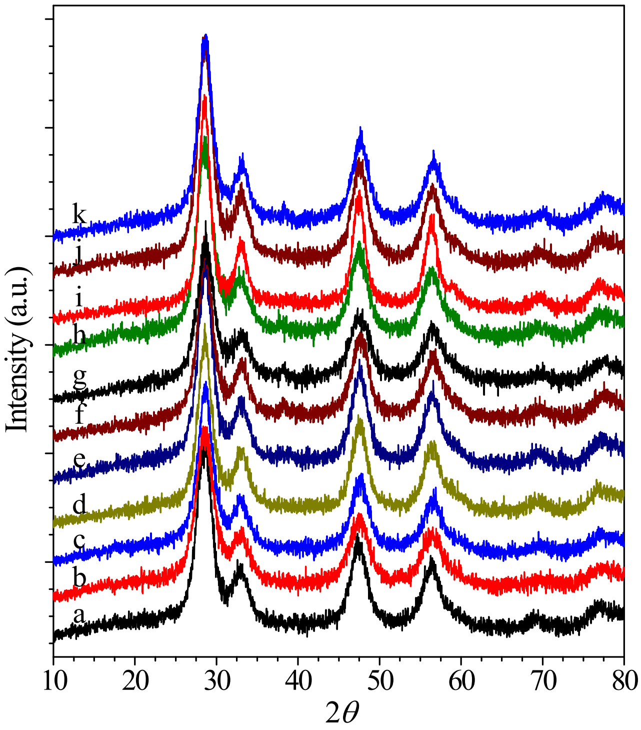

Fig. S12 XRD patterns of 2D ceria doped with other metal oxides: (a) NS-CeCo; (b) NS-CeCr; (c) NS-CeCu; (d) NS-CeFe; (e) NS-CeMn; (f) NS-CeNi; (g) NS-CeTi; (h) NS-CeZn; (i) NS-CeZr; (j) NS-CeLa; and (k) NS-CeAl. The molar ratio of Ce/M is 8.

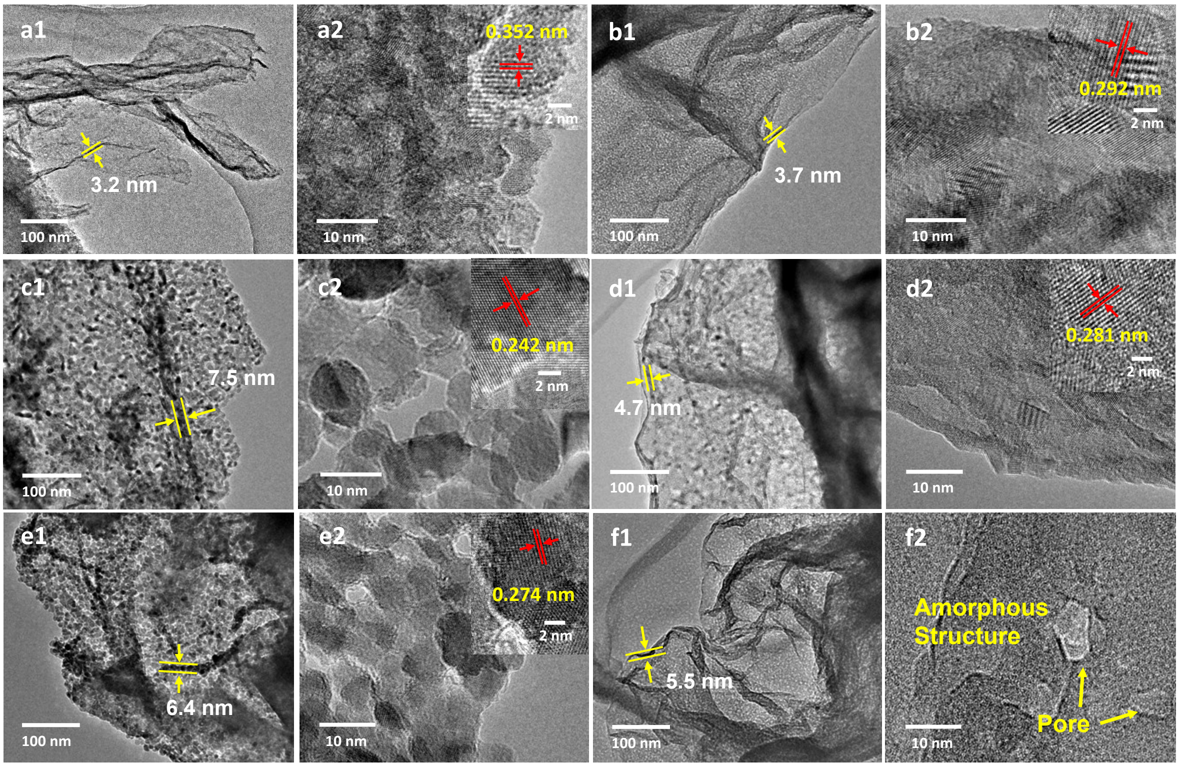

Fig. S13 TEM images of various 2D single metal oxides nanosheets: (a1, a2) NS-TiO_2; (b1, b2) NS-ZrO_2; (c1, c2) NS-NiO; (d1, d2) NS-CoO_x; (e1, e2) NS-CuO; and (f1, f2) NS-Al_2O_3.

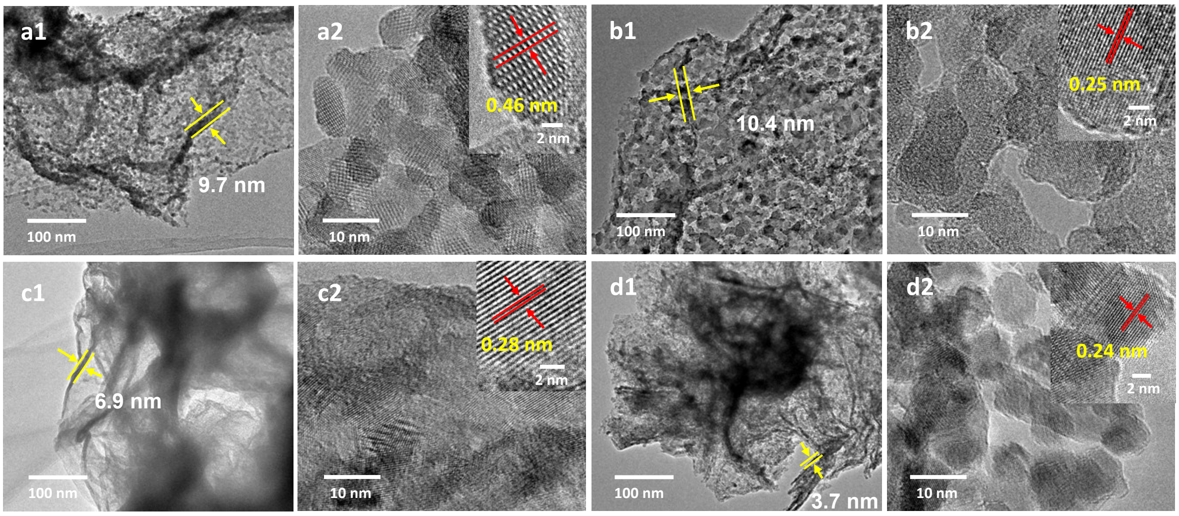

Fig. S14 TEM images of various 2D binary metal oxides nanosheets: (a1, a1) Cr_2O_3-ZnO; (b1, b2) MnO_x-Al_2O_3; (c1, c2) CuO-ZrO_2; and (d1, d2) FeO_x-CoO_x.

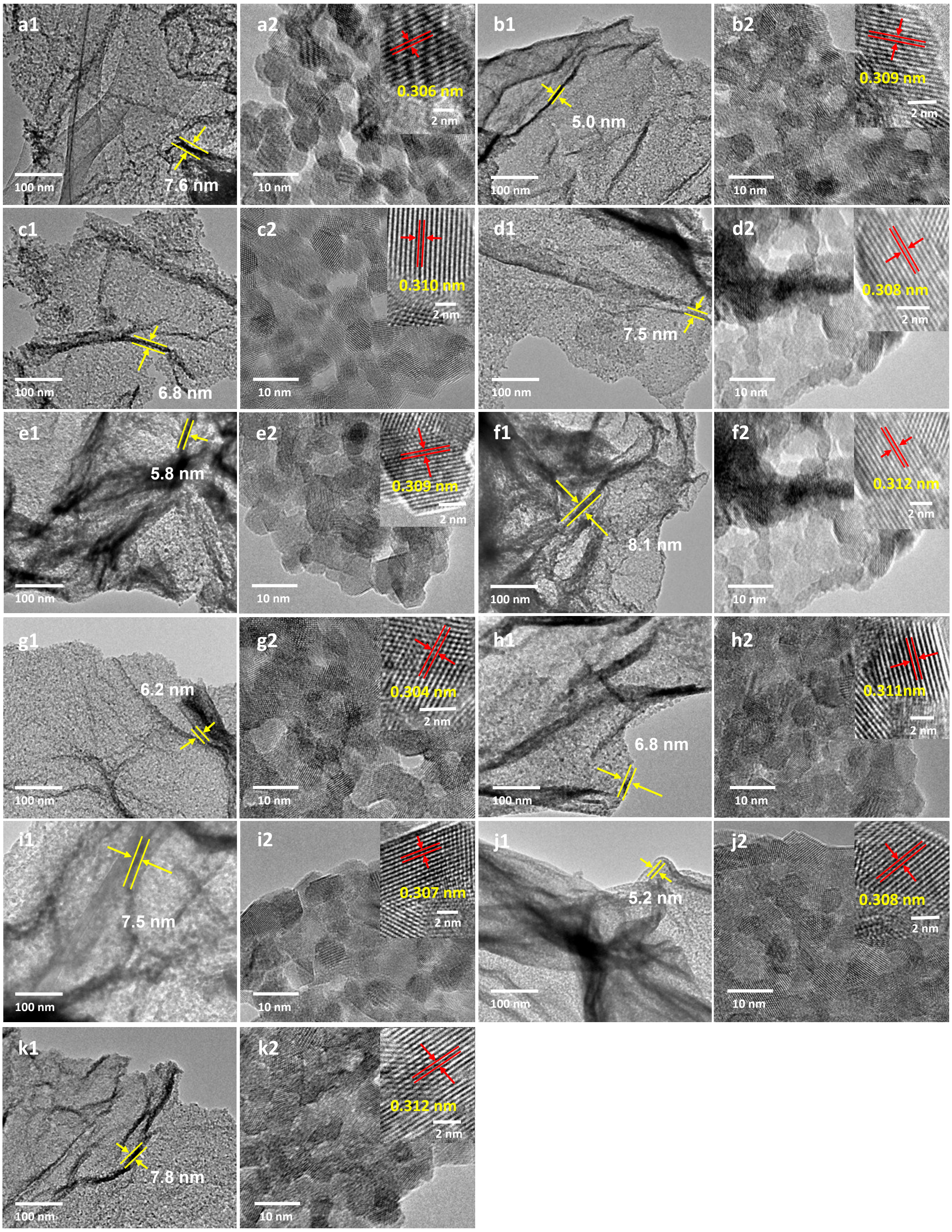

Fig. S15 TEM images of various 2D ceria nanosheets doped with other metal oxides: (a1, a2) CeO_2-CoO_x; (b1, b2) CeO_2-Cr_2O_3; (c1, c2) CeO_2-CuO; (d1, d2) CeO_2-FeO_x; (e1, e2) CeO_2-MnO_x; (f1, f2) CeO_2-NiO; (g1, g2) CeO_2-TiO_2; (h1, h2) CeO_2-ZnO; (i1, i2) CeO_2-ZrO_2; (j1, j2) CeO_2-La_2O_3; and (k1, k2) CeO_2-Al_2O_3.

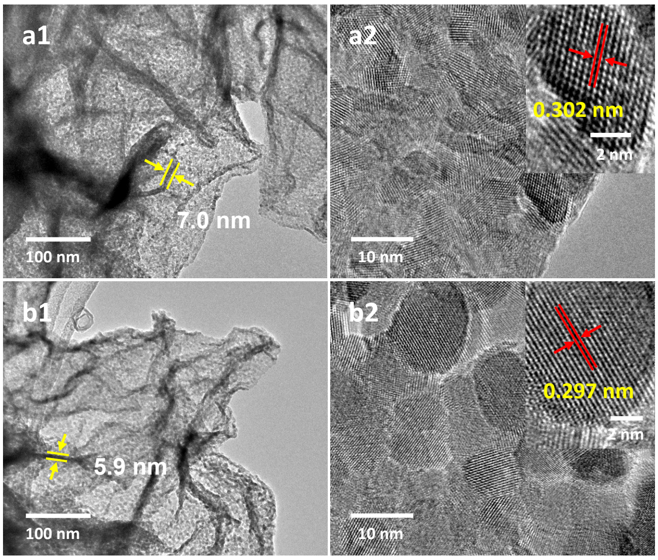

Fig. S16 TEM images of various 2D ternary metal oxides nanosheets: (a1, a2) CuO-CeO_2-ZrO_2; and (b1, b2) MnO_x-CeO_2-ZrO_2.

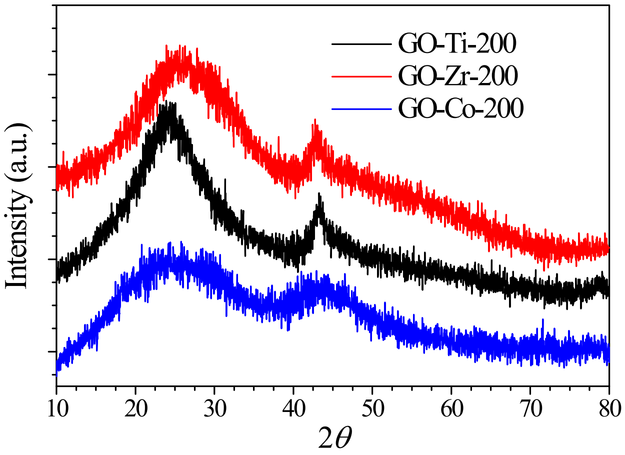

Fig. S17 XRD patterns of different GO-metal complexes annealed at 200 °C.

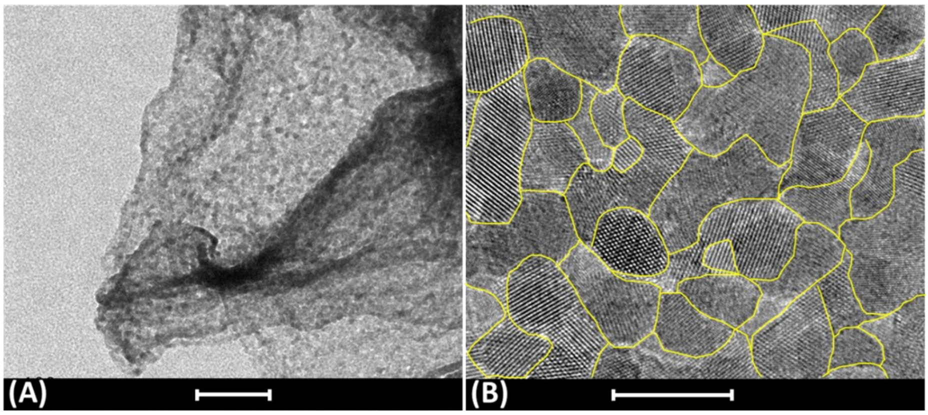

Fig. S18 TEM (A) and high-resolution TEM (B) images of the Pd/NS-CeO_2-catalyst. Scale bar: (A) 100 nm, (B) 10 nm.

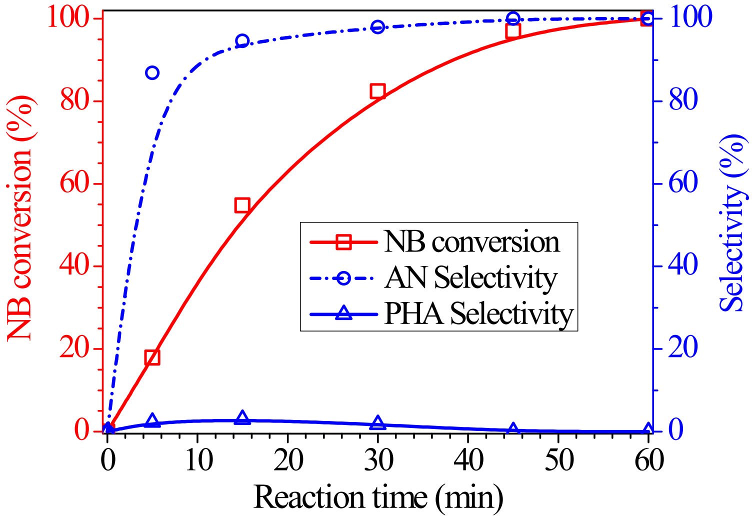

Fig. S19 Evolution of the conversion of nitrobenzene (NB) and selectivity to N-phenylhydroxylamine (PHA) and aniline (AN) with the reaction time for NB hydrogenation over Pd/NS-CeO_2-450. Reaction conditions: 5 mg catalyst, 5 mL methanol, 0.2 MPa H_2, and 25 °C; the molar ratio of NB to Pd was about 1300.

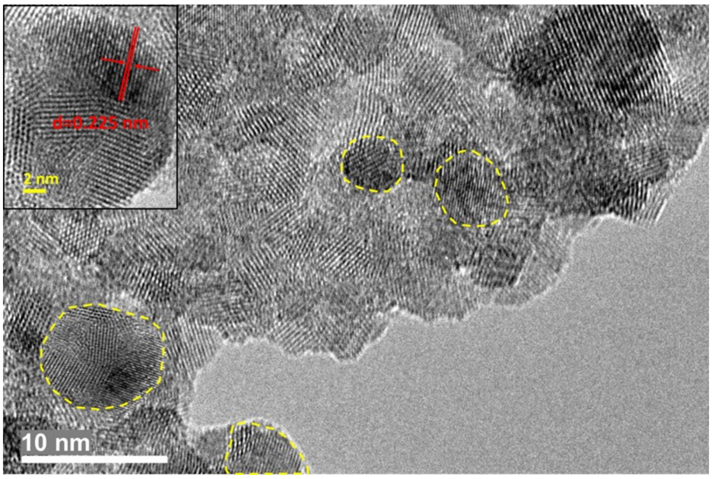

Fig. S20 High-resolution TEM image of the Pd-IM/NS-CeO_2-catalyst.

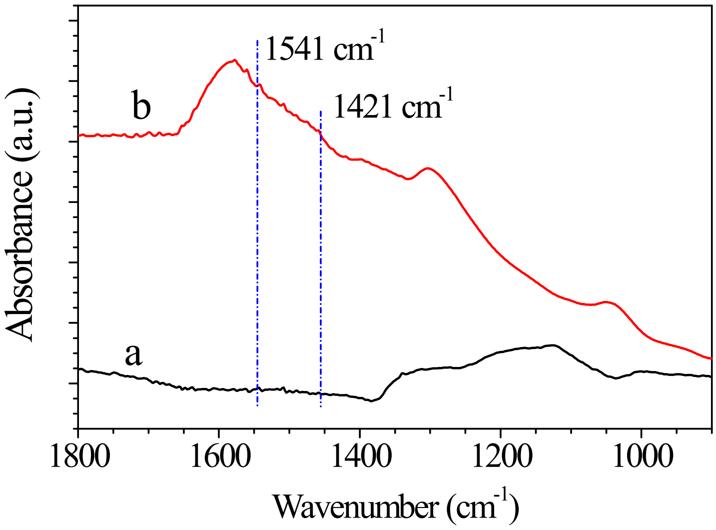

Fig. S21 FT-IR spectra of the NS-CeO_2-450 support before (a) and after (b) the adsorption of nitrobenzene.

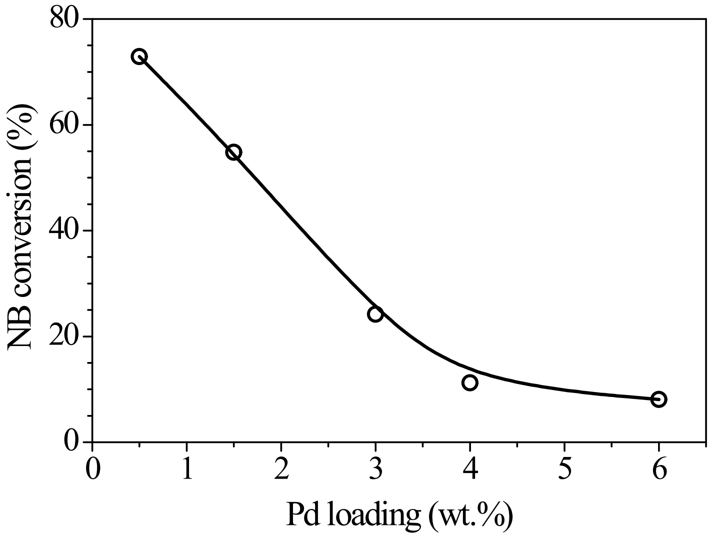

Fig. S22 Effect of Pd loading on the conversion of nitrobenzene (NB) for NB hydrogenation over Pd/NS-CeO$_2$-450. Reaction conditions: 5 mL methanol, 0.2 MPa H$_2$, and 25 °C; the weight of Pd/NS-CeO$_2$-450 catalyst added in the autoclave reactor was adjusted to ensure that the molar ratio of NB to Pd was about 1300; the NB conversions were acquired after reaction for 15 min.

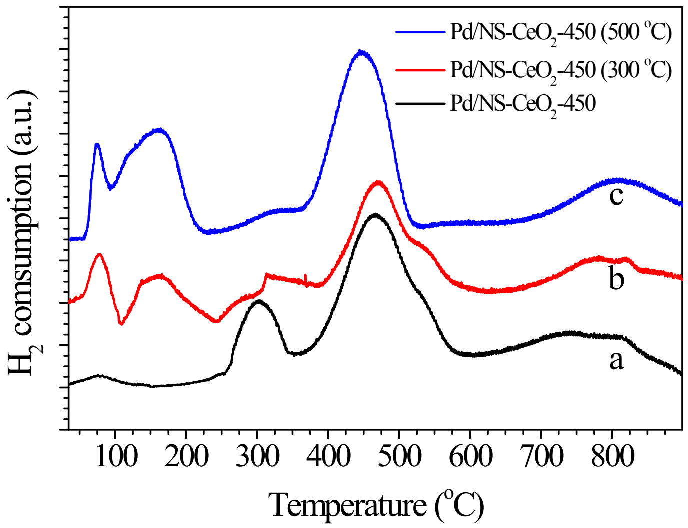

Fig. S23 H$_2$-TPR profiles of various Pd/NS-CeO$_2$ catalysts: (a) fresh Pd/NS-CeO$_2$-450; (b) Pd/NS-CeO$_2$-450 (300 °C), upon calcining treatment at 300 °C; and (c) Pd/NS-CeO$_2$-450 (500 °C), upon calcining at 500 °C.

Reference

(1) C. Chen, Q. H. Yang, Y. Yang, W. Lv, Y. Wen, P. X. Hou, M. Wang and H. M. Cheng, *Adv. Mater.*, 2009, **21**, 3007–3011.

(2) S. Li, H. Zhu, Z. Qin, G. Wang, Y. Zhang, Z. Wu, Z. Li, G. Chen, W. Dong, Z. Wu, L. Zheng, J. Zhang, T. Hu and J. Wang, *Appl. Catal., B*, 2014, **144**, 498–506.

(3) F. A. Harraz, S. E. El-Hout, H. M. Killa and I. A. Ibrahim, *J. Catal.*, 2012, **286**, 184–192.

(4) S. Samanta and A. K. Nandi, *J. Phys. Chem. C*, 2009, **113**, 4721–4725.

(5) G. Q. Kong, S. Ou, C. Zou and C. D. Wu, *J. Am. Chem. Soc.*, 2012, **134**, 19851–19857.

(6) O. Verho, K. J. Gustafson, A. Nagendiran, C. W. Tai and J. E. Bäckvall, *ChemCatChem*, 2014, **6**, 3153–3159.

(7) F. Zhang, J. Jin, X. Zhong, S. Li, J. Niu, R. Li and J. Ma, *Green Chem.*, 2011, **13**, 1238–1243.

(8) Q. Yang, Y. Z. Chen, Z. U. Wang, Q. Xu and H. L. Jiang, *Chem. Commun.*, 2015, **51**, 10419–10422.

(9) K. Xu, Y. Zhang, X. Chen, L. Huang, R. Zhang and J. Huang, *Adv. Synth. Catal.*, 2011, **353**, 1260–1264.

(10) M. M. Dell'Annaa, S. Intinia, G. Romanazzia, A. Rizzutia, C. Leonellib, F. Piccinnia and P. Mastrorillia, *J. Mol. Catal. A: Chem.*, 2014,**395**, 307–314.

(11) V. Pandarus, R. Ciriminna, F. Béland and M. Pagliaro, *Adv. Synth. Catal.*, 2011, **353**, 1306–1316.

(12) H. Yang, X. Cui, Y. Deng and F. Shi, *ChemCatChem*, 2013, **5**, 1739–1743.